

Transmission properties of left-handed band-gap structures

Ilya V. Shadrivov¹, Nina A. Zharova^{1,2}, Alexander A. Zharov^{1,3}, and Yuri S. Kivshar¹¹ Nonlinear Physics Group and Centre for Ultra-high bandwidth Devices for Optical Systems (CUDOS),
Research School of Physical Sciences and Engineering,
Australian National University, Canberra ACT 0200, Australia² Institute of Applied Physics, Russian Academy of Sciences, Nizhny Novgorod 603600, Russia³ Institute for Physics of Microstructures, Russian Academy of Sciences, Nizhny Novgorod 603950, Russia

We analyze transmission of electromagnetic waves through a periodic band-gap structure consisting of slabs of a left-handed metamaterial and air. Using the effective parameters of the metamaterial derived from its microscopic structure, we study, with the help of the transfer-matrix approach and by means of the finite-difference time-domain numerical simulations, the transmission properties of such a left-handed photonic crystal in a novel type of band gap associated with the zero averaged refractive index. We demonstrate that the transmission can be made tunable by introducing defects, which allow to access selectively two different types of band gaps.

PACS numbers: 42.70.Qs, 41.20.Jb, 78.20.-e

I. INTRODUCTION

Materials with both negative dielectric permittivity and negative magnetic permeability were suggested theoretically a long time ago [1], and they are termed left-handed materials because the wave vector and Poynting vector lie in the opposite directions. Many unusual properties of such materials can be associated with their negative refractive index, as was demonstrated by several reliable experiments [2, 3] and numerical finite-difference time-domain (FDTD) simulations (see, e.g., Ref. [4]).

Multilayered structures that include materials with negative refraction can be considered as a sequence of the flat lenses that provide an optical cancellation of the layers with positive refractive index leading to either enhanced or suppressed transmission [5, 6, 7]. More importantly, a one-dimensional stack of layers with alternating positive and negative-refraction materials with zero averaged refractive index displays a novel type of the transmission band gap [6, 8, 9, 10, 11] near the frequency where the condition $\langle n \rangle = 0$ is satisfied; such a novel band gap is quite different from a conventional Bragg reflection gap because it appears due to completely different physics of wave reflection. In particular, the periodic structures with zero averaged refractive index demonstrate a number of unique properties of the beam transmission observed as strong beam modification and reshaping [8] being also insensitive to disorder that is symmetric in the random variable [9].

In this paper, we study both transmission properties and defect-induced tunability of the left-handed photonic band gap structures created by alternating slabs of positive and negative refractive index materials with an embedded defect taking into account realistic parameters, dispersion and losses of the left-handed material. We consider a band-gap structure schematically shown in Fig. 1. First, we study the properties of the left-handed material as a composite structure made of arrays of wires and split-ring resonators (see the insert in Fig. 1) and derive the general results for the effective dielectric per-

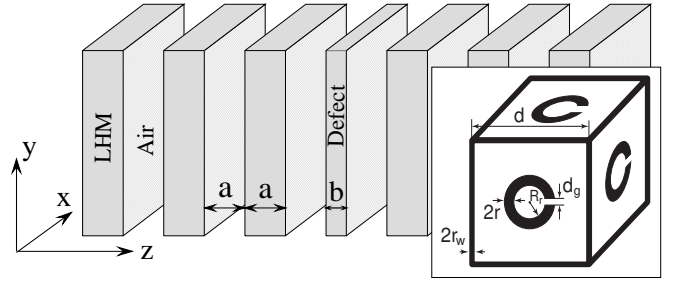


FIG. 1: Schematic of a multilayered structure consisting of alternating metamaterial slabs and air. The inset shows the unit cell of the metamaterial structure.

mittivity and magnetic permeability. Second, we study the transmission of electromagnetic waves through the layered structure consisting of alternating slabs of composite left-handed metamaterial using the calculated effective parameters. We assume that the structure includes a defect layer (see Fig. 1) that allows tunability of the transmission near the defect frequency. Using the transfer-matrix method, we describe the defect-induced localized states in such a structure and reveal that the defect modes may appear in different parameter regions and for both $\langle n \rangle = 0$ and Bragg scattering band gaps. Depending on the defect parameters, the maximum transmission can be observed in all or just some spectral band gaps of the structure. We demonstrate that the frequency of the defect mode is less sensitive to manufacturing disorder for the larger defect layer. Finally, we perform two-dimensional FDTD numerical simulations based on the microscopic parameters of the left-handed material and study the temporal evolution of the transmitted and reflected fields.

II. METAMATERIAL CHARACTERISTICS

We assume that the left-handed metamaterial is created by a three-dimensional lattice of wires and splitting resonators (SRRs), as shown in the inset of Fig. 1. According to the results of the derivation presented in Refs. [12, 13], the main contribution to the effective dielectric permittivity of this structure is given by the wires, whereas the magnetic response is determined by SRRs. Although a three-dimensional lattice of wires contains closed circuits, we neglect their contribution to the magnetic permeability, because this effect is non-resonant, and, therefore, is weak. The effective dielectric permittivity can be obtained in the form [12, 13]

$$\epsilon(\omega) = 1 - \frac{\omega_p^2}{\omega(\omega + i\gamma)}; \quad (1)$$

where $\omega_p = \sqrt{4\pi n_m} \left[\frac{c}{d} \ln \left(\frac{d}{r_w} \right) \right]^{1/2}$ is the effective plasma frequency, $\gamma = \frac{c^2}{2S} \ln \left(\frac{d}{r_w} \right)$, S is the wire conductivity, S is the effective cross-section of a wire, $S = \frac{\pi r_w^2}{2}$, for $\omega > \frac{c}{d} \ln \left(\frac{d}{r_w} \right)$, and $S = \frac{\pi r_w^2}{2} \left(\frac{2r_w}{d} \right)$, for $\omega < \frac{c}{d} \ln \left(\frac{d}{r_w} \right)$, where $\frac{c}{d} \ln \left(\frac{d}{r_w} \right)$ is the skin-layer thickness.

To calculate the effective magnetic permeability of the lattice of SRRs we write its magnetization M in the form (see also Ref. [14])

$$M = (n_m = 2c) R_r^2 I_r; \quad (2)$$

where $n_m = 3/d^3$ is the number of SRRs per unit cell, R_r is the SRR radius (see the insert in Fig. 1), I_r is the current in the SRR. We assume that SRR is an effective oscillatory circuit with inductance L and resistance R of the wire, and capacity C of the SRR slot. In this circuit the electromotive force in this circuit due to an alternating magnetic field of the propagating wave. Under these assumptions, the evolution of the current I_r in single SRR is governed by the equation

$$L \frac{d^2 I_r}{dt^2} + R \frac{dI_r}{dt} + \frac{1}{C} I_r = \frac{dE}{dt}; \quad (3)$$

with

$$E = \frac{R_r^2}{c} \frac{dH^0}{dt};$$

where H^0 is the acting (microscopic) magnetic field, which differs from the average (macroscopic) magnetic field. We describe the SRR array as a system of magnetic dipoles, which is valid when the number of SRRs in the volume V is big enough, and use the Lorenz-Lorentz relation between the microscopic and macroscopic magnetic fields [15]

$$H^0 = H + \frac{4}{3} M = B - \frac{8}{3} M; \quad (4)$$

As a result, from Eqs. (2)-(4) we obtain the effective magnetic permeability of the structure in the form,

$$\mu(\omega) = 1 + \frac{F \omega^2}{\omega_0^2 (1 + F = 3) + i\gamma}; \quad (5)$$

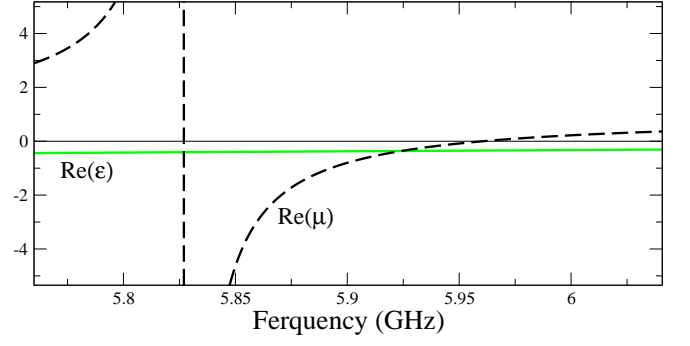


FIG. 2: Frequency dependence of the real part of the dielectric permittivity $\text{Re}(\epsilon)$ (solid), and the real part of magnetic permeability $\text{Re}(\mu)$ (dashed).

where $F = 2 n_m (R_r^2/c)^2 = L$, $\omega_0^2 = 1/LC$, and $\gamma = R/L$. Inductance L , resistance R , and capacitance C are given by the following results (see, e.g., Ref. [16]),

$$L = \frac{4 R_r}{c^2} \ln \frac{8R_r}{r} - \frac{7}{4}; \quad R = \frac{2 R_r}{S_r}; \quad C = \frac{r^2}{4 d_g};$$

where r is the radius of the wire that makes a ring, σ is conductivity of the wire, S_r is the effective area of the cross-section of SRR wire defined similar to that of a straight wire, and d_g is the size of the SRR slot. We note, that the result for C should hold provided $d_g \gg r$.

Taking the parameters of a metallic composite as $d = 1$ cm, $r_w = 0.05$ cm, $R_r = 0.2$ cm, $r = 0.02$ cm, $d_g = 10^{-3}$ cm, and its conductivity as $\sigma = 2 \cdot 10^8$ s⁻¹, we calculate the effective frequency dependencies of $\epsilon(\omega)$ and $\mu(\omega)$ according to Eqs. (1) and (5), respectively, and show these dependencies in Fig. 2. The resonance frequency appears near 5.82 GHz, and the region of simultaneously negative ϵ and μ is between 5.82 GHz and 5.96 GHz. The imaginary part of the magnetic permeability, which determines effective losses in a left-handed material, is larger near the resonance.

III. TRANSMISSION AND DEFECT MODES

We consider now a band gap structure created by seven alternating left-handed and dielectric slab pairs, as shown in Fig. 1. The number of slabs is chosen to keep losses in the structure at a reasonably low level, still having visible the effects of periodicity. We assume that the periodic structure is created by slabs of the width a , made of the left-handed composite described above, and separated by air ($\epsilon_a = 1$, $\mu_a = 1$). The middle layer of the left-handed material is assumed to have a different thickness, $b = a(1 + \delta)$, in order to describe a structural defect.

To study the transmission characteristics of such a band-gap structure, we consider a normal-incidence plane wave for the scalar electric field described by the

Helmholtz-type equation,

$$\frac{d^2}{dz^2} + \frac{\epsilon^2}{c^2} \epsilon(z) \epsilon(z) - \frac{1}{\epsilon(z)} \frac{d}{dz} \frac{d}{dz} E = 0; \quad (6)$$

where $\epsilon(z)$ and $\epsilon(z)$ are the dielectric permittivity and magnetic permeability in the whole space.

Before analyzing the transmission properties of a finite layered structure, first we study the corresponding infinite structure without defects and calculate its band gap spectrum. In an infinite periodic structure, propagating waves in the form of the Floquet-Bloch modes satisfy the periodicity condition, $E(z + 2a) = E(z) \exp(2iaK_b)$, where K_b is the Bloch wavenumber. The values of K_b are found as solutions of the standard eigenvalue equation for a two-layered periodic structure (see, e.g., Ref. [11]),

$$2 \cos(K_b 2a) = 2 \cos[(k_r + k_l)a] \\ \frac{p_r}{p_l} + \frac{p_l}{p_r} = 2 \sin \phi(a) \sin \phi(a); \quad (7)$$

where $p_r = 1$, $p_l = \frac{p}{c} = \frac{p}{c}$, $k_r = \frac{\omega}{c}$ and $k_l = \frac{\omega}{c} \frac{p}{c}$ are the wavevectors in air and left-handed slabs, respectively. For real values of K_b , the Bloch waves are propagating; complex values of K_b indicate the presence of band gaps, where the wave propagation is suppressed. The spectral gaps appear when the argument of the cosine function in Eq. (7) becomes the whole multiple of π , and no real solutions for K_b exist. These gaps are usually termed as Bragg gaps. The presence of the left-handed material in the structure makes it possible for the argument to vanish, so that the wave propagation becomes prohibited in this case as well, thus creating an additional band gap, which do not exist in conventional periodic structures. As a matter of fact, the condition $|k_r| = |k_l|$ corresponds to the zero average refractive index, $\langle n \rangle = 0$, as discussed in Refs. [6, 8, 9, 10, 11]. However, the inherent feature of the left-handed materials is their frequency dispersion, so that the condition $|k_r| = |k_l|$ defines a characteristic frequency ω at which the indices of refraction in both the media compensate each other. In a sharp contrast to the conventional Bragg reflection gaps, the position of this additional $\langle n \rangle = 0$ gap in the frequency domain does not depend on the optical period of the structure.

For the parameters of the left-handed media described above, the frequency ω at which the average refractive index vanishes is found as $\omega = 2\pi \times 5.8636 \text{ GHz}$. Importantly, the transmission coefficient calculated at $\omega = \omega$ for the seven-layer structure shows a characteristic resonant dependence as a function of the normalized slab thickness a/λ , where $\lambda = 2\pi c/\omega$, as shown in Fig. 3. The transmission maxima appear in the $\langle n \rangle = 0$ gap, when the slab thickness a coincides with a whole multiple of a half of the wavelength. The width of the transmission peaks decreases with the increase of the number of layers in the structure. The transmission maxima decrease with increasing thickness of the structure due to losses in the left-handed material which become larger for thicker slabs. One of the interesting features of the $\langle n \rangle = 0$

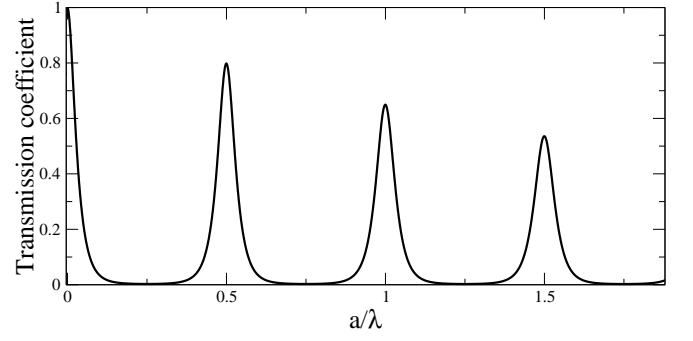


FIG. 3: Transmission coefficient of a finite periodic structure with seven layers of left-handed material vs. the normalized slab thickness a/λ , where $\lambda = 2\pi c/\omega$ and the frequency $\omega = \omega$ corresponds to the condition $\langle n \rangle = 0$.

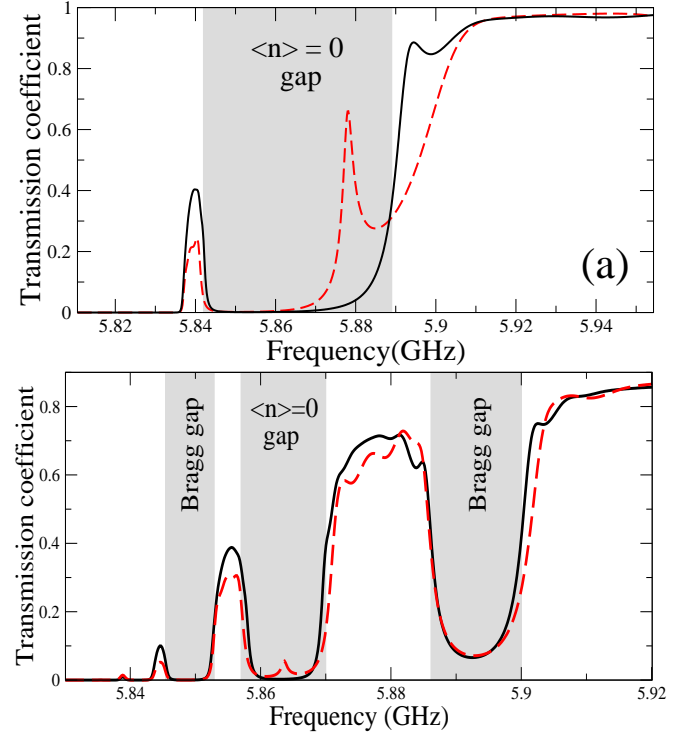


FIG. 4: Transmission coefficient of the left-handed band-gap structure vs. the wave frequency. (a) The structure with the period $a = 0.25$, without (solid) and with (dashed) defect layer ($\epsilon = 0.8$). (b) The structure with the period $a = 1.25$ without (solid) and with (dashed) defect layer ($\epsilon = 0.6$).

gap is that the transmission coefficient can vanish even for very small values of the slab thickness. This property can be employed to create effective mirrors in the microwave region operating in this novel $\langle n \rangle = 0$ gap which can be effectively thinner than the wavelength of electromagnetic waves.

The transmission coefficient is shown in Fig. 4 (a,b) as a function of the frequency, for two structures with different values of the period a . For the quarter-wavelength

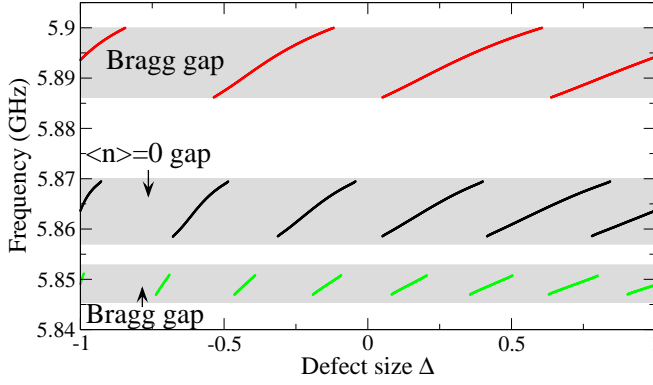


FIG. 5: Frequency spectrum of the defect modes as a function of the normalized defect size in the left-handed band-gap structure with the period $a = 1.25$.

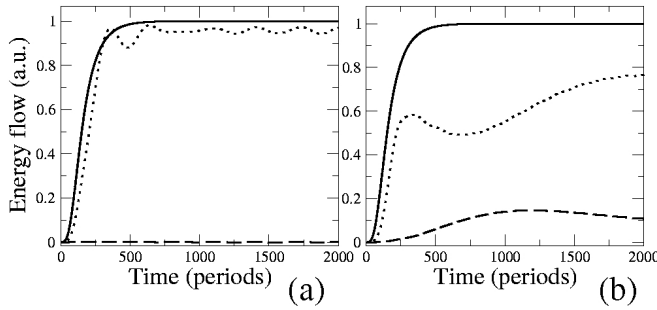


FIG. 6: Numerical FDTD simulation results showing relaxation processes in a band-gap structure with a defect. Solid { incident energy flow, dashed { transmitted energy flow, dotted { reflected energy flow. Parameters are: $a = 0.25$, $\epsilon = 0.8$. (a) Defect mode is not excited, $\omega = 2.586 \cdot 10^9 \text{ s}^{-1}$; (b) Defect mode is excited, $\omega = 2.5878 \cdot 10^9 \text{ s}^{-1}$.

slabs [see Fig. 4(a)], the only visible band gap is the $\langle n \rangle = 0$ gap centered near ω where both ϵ and μ are negative. When the structure has a defect, the transmission peak associated with the excitation of the defect mode appears inside the $\langle n \rangle = 0$ gap as shown by the dashed curve. For the structure with thicker slabs, e.g. for $a = 1.25$ [see Fig. 4(b)] the $\langle n \rangle = 0$ gap becomes narrower but it remains centered near the frequency ω . The transmission coefficient of this second band-gap structure shows, in addition to the $\langle n \rangle = 0$ gap, two Bragg scattering gaps. Due to the increased losses in this second band-gap structure, where slabs are thicker than in the structure corresponding to Fig. 4(a), the effects of the resonant transmission at the defect mode become less visible. Moreover, for the parameters we consider here the defect mode appears only in the $\langle n \rangle = 0$ gap, whereas it does not appear in the Bragg gaps. For larger slab thickness, higher-order Bragg gaps may appear in the frequency range where the composite material is left-handed.

In Fig. 5, we show the frequency spectrum of the defect modes for the structure with $a = 1.25$ as a function of the normalized defect size Δ . We notice a number of

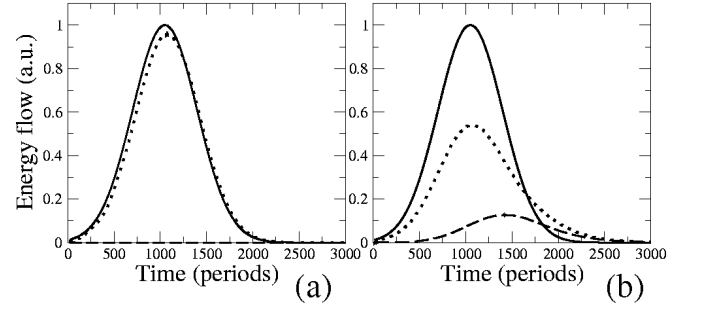


FIG. 7: Numerical FDTD simulation results for the pulse scattering by a periodic structure with defect. Solid { incident energy flow, dashed { transmitted energy flow, dotted { reflected energy flow. Parameters are: $a = 0.25$, $\epsilon = 0.8$. (a) Defect mode is not excited, $\omega = 2.586 \cdot 10^9 \text{ s}^{-1}$; (b) Defect mode is excited, $\omega = 2.5878 \cdot 10^9 \text{ s}^{-1}$.

important features: (i) the defect modes do not always appear simultaneously in all gaps, and (ii) the slope of the curves in Fig. 5 decreases with the growth of the defect thickness. As a result, the eigenfrequencies of the modes introduced by thicker defect layers can be more stable to disorder introduced by manufacturing. These novel features seem to be important for tunable properties of the layered structures because the different modes allow to access different types of band gaps.

IV. NUMERICAL FDTD SIMULATIONS

In order to analyze the temporal evolution of the transmitted fields and the beam scattering under realistic conditions, we perform two-dimensional FDTD numerical simulations of the beam propagation through the left-handed periodic structure of seven layers with a defect. We consider TM-polarized Gaussian beam of the width 20 propagating towards the structure with the period $a = 0.25$; such a structure corresponds to the transmission coefficient shown in Fig. 4(a) by a dashed line. First, we choose the frequency of the incident field in the $\langle n \rangle = 0$ gap. The temporal evolution of the energy flows (integrated over the transverse dimension) for the incident, transmitted, and reflected waves is shown in Fig. 6(a), clearly indicating that the transmission through such a structure is negligible. When the frequency of the incident field coincides with that of the defect mode, a significant amount of the energy is transmitted through the structure [see Fig. 6(b)]. The relaxation time of the beam transmission through the structure is estimated as 10^3 periods (approximately 170 ns).

Results of FDTD simulations for the pulse scattering from the structure with $a = 0.25$ are shown in Figs. 7(a,b) as the temporal dependence of the incident, reflected and transmitted energy flows. One can clearly see significant transmission, when the carrier frequency of the pulse coincides with the eigen frequency of the defect mode [see Figs. 7(a,b)].

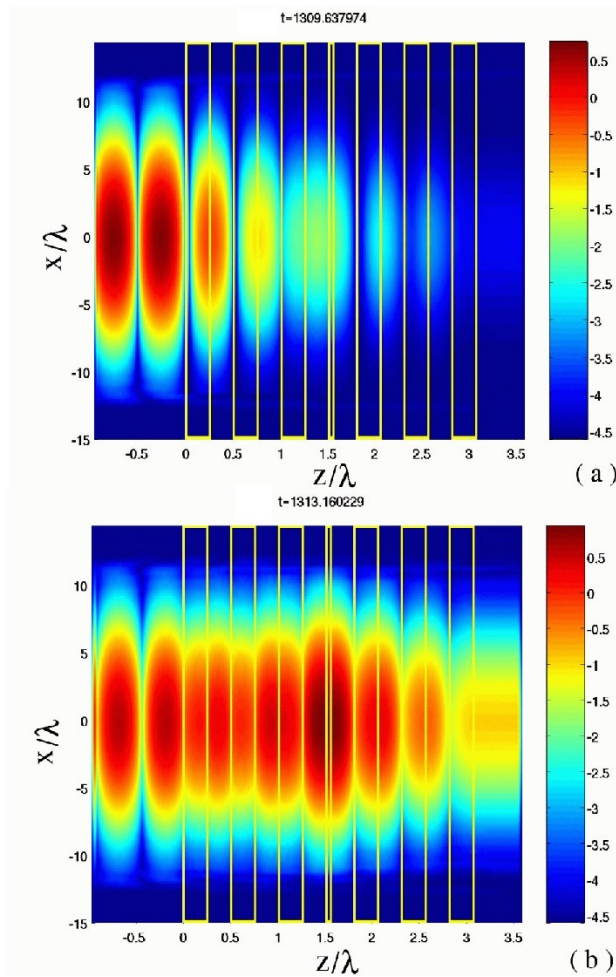


FIG. 8: Results of the numerical FDTD simulations for the amplitude of the magnetic field in a two-dimensional structure (natural logarithm scale). Boxes show positions of the left-handed slabs, $a = 0.25$, $b = 0.8$. (a) Defect mode is not excited, $\omega = 2.586 \times 10^9 \text{ s}^{-1}$; (b) Defect mode is excited, $\omega = 2.5878 \times 10^9 \text{ s}^{-1}$.

An example of the field distribution in the structure with the slab size $a = 0.25$ is shown in Figs. 8 (a,b) for two different regimes. In Fig. 8(a), the frequency corresponds to low transmission in Fig. 4(a), when no defect mode is excited. Figure 8(b) demonstrates the field distribution in the structure with an excited defect mode and enhanced transmission.

V. CONCLUSIONS

We have studied the transmission properties of periodic structures made of a left-handed metamaterial and air. Using realistic parameters of the metamaterial derived from the microscopic approach, we have calculated the band-gap spectrum of an infinite one-dimensional structure with and without defects, demonstrating the existence of band gaps of two different types, the conventional Bragg scattering gaps and a novel $\langle n \rangle = 0$ gap. We have analyzed the properties of the defect modes in a finite periodic structure with a structural defect and demonstrated that, depending on the defect size, the defect modes appear in all or just some of the band gaps allowing to access different gaps selectively. In addition, we have performed two-dimensional numerical FDTD simulations of the propagation of electromagnetic waves in such structures and have studied the temporal dynamics of the beam transmission and reflection. We have demonstrated that the excitation of defect modes can enhance substantially the wave transmission through the structure.

The authors thank Michael Feise for collaboration, and acknowledge a partial support from the Australian Research Council.

-
- [1] V. G. Veselago, *Usp. Fiz. Nauk* 92, 517 (1967) (in Russian) [*Phys. Usp.* 10, 509 (1968)].
 - [2] R. A. Shelby, D. R. Smith, and S. Schultz, *Science* 292, 77 (2001).
 - [3] C. G. Parazzoli, R. B. Gregor, K. Li, B. E. C. Koltenbah, and M. Tanielian, *Phys. Rev. Lett.* 90, 107401 (2003).
 - [4] S. Foteinopoulou, E. N. Economou, and C. M. Soukoulis, *Phys. Rev. Lett.* 90, 107402 (2003).
 - [5] J. B. Pendry and S. A. Ramakrishna, *J. Phys. Condens. Matter* 15, 6345 (2003).
 - [6] I. S. Nefedov and S. A. Tretyakov, *Phys. Rev. E* 66, 036611 (2002).
 - [7] Z. M. Zhang and C. J. Fu, *Appl. Phys. Lett.* 80, 1097 (2002).
 - [8] I. V. Shadrivov, A. A. Sukhorukov, and Yu. S. Kivshar, *Appl. Phys. Lett.* 82, 3820 (2003).
 - [9] J. Li, L. Zhou, C. T. Chan, and P. Sheng, *Phys. Rev. Lett.* 90, 083901 (2003).
 - [10] R. Ruppin, *Microsc. Opt. Technol. Lett.* 38, 494 (2003).
 - [11] L. Wu, S. L. He, and L. F. Shen, *Phys. Rev. B* 67, 235103 (2003).
 - [12] J. B. Pendry, A. J. Holden, W. J. Stewart, and I. Youngs, *Phys. Rev. Lett.* 76, 4773 (1996).
 - [13] A. A. Zharov, I. V. Shadrivov, and Yu. S. Kivshar, *Phys. Rev. Lett.* 91, 037401 (2003).
 - [14] J. B. Pendry, A. J. Holden, D. J. Robbins, and W. J. Stewart, *IEEE Trans. Microw. Theory Tech.* 47, 2075 (1999).
 - [15] L. D. Landau and E. M. Lifshitz, *Electrodynamics of Continuous Media* (Pergamon Press, Oxford, 1963).
 - [16] J. Schwinger, *Classical Electrodynamics* (Perseus Books, Reading, Mass., 1998).